AMERICAN SOCIETY FOR MICROBIOLOGY | mBio®

RESEARCH ARTICLE

A *Pseudomonas aeruginosa* Antimicrobial Affects the Biogeography but Not Fitness of *Staphylococcus aureus* during Coculture

Juan P. Barraza,[a,b,c] **Marvin Whiteley**[a,b,c]

[a]School of Biological Sciences, Georgia Institute of Technology, Atlanta, Georgia, USA
[b]Center for Microbial Dynamics and Infection, Georgia Institute of Technology, Atlanta, Georgia, USA
[c]Emory–Children's Cystic Fibrosis Center, Atlanta, Georgia, USA

ABSTRACT *Pseudomonas aeruginosa* and *Staphylococcus aureus* are two of the most common coinfecting bacteria in human infections, including the cystic fibrosis (CF) lung. There is emerging evidence that coinfection with these microbes enhances disease severity and antimicrobial tolerance through direct interactions. However, one of the challenges to studying microbial interactions relevant to human infection is the lack of experimental models with the versatility to investigate complex interaction dynamics while maintaining biological relevance. Here, we developed a model based on an *in vitro* medium that mimics human CF lung secretions (synthetic CF sputum medium [SCFM2]) and allows time-resolved assessment of fitness and community spatial structure at the micrometer scale. Our results reveal that *P. aeruginosa* and *S. aureus* coexist as spatially structured communities in SCFM2 under static growth conditions, with *S. aureus* enriched at a distance of 3.5 μm from *P. aeruginosa*. Multispecies aggregates were rare, and aggregate (biofilm) sizes resembled those in human CF sputum. Elimination of *P. aeruginosa*'s ability to produce the antistaphylococcal small molecule HQNO (2-heptyl-4-hydroxyquinoline *N*-oxide) had no effect on bacterial fitness but altered the spatial structure of the community by increasing the distance of *S. aureus* from *P. aeruginosa* to 7.6 μm. Lastly, we show that coculture with *P. aeruginosa* sensitizes *S. aureus* to killing by the antibiotic tobramycin compared to monoculture growth despite HQNO enhancing tolerance during coculture. Our findings reveal that SCFM2 is a powerful model for studying *P. aeruginosa* and *S. aureus* and that HQNO alters *S. aureus* biogeography and antibiotic susceptibility without affecting fitness.

IMPORTANCE Many human infections result from the action of multispecies bacterial communities. Within these communities, bacteria have been proposed to directly interact via physical and chemical means, resulting in increased disease and antimicrobial tolerance. One of the challenges to studying multispecies infections is the lack of robust, infection-relevant model systems with the ability to study these interactions through time with micrometer-scale precision. Here, we developed a versatile *in vitro* model for studying the interactions between *Pseudomonas aeruginosa* and *Staphylococcus aureus*, two bacteria that commonly coexist in human infections. Using this model along with high-resolution, single-cell microscopy, we showed that *P. aeruginosa* and *S. aureus* form communities that are spatially structured at the micrometer scale, controlled in part by the production of an antimicrobial by *P. aeruginosa*. In addition, we provide evidence that this antimicrobial enhances *S. aureus* tolerance to an aminoglycoside antibiotic only during coculture.

KEYWORDS *Pseudomonas aeruginosa*, *Staphylococcus aureus*, model, HQNO, spatial structure, cystic fibrosis, SCFM2, biogeography, coculture, model system

Citation Barraza JP, Whiteley M. 2021. A *Pseudomonas aeruginosa* antimicrobial affects the biogeography but not fitness of *Staphylococcus aureus* during coculture. mBio 12:e00047-21. https://doi.org/10.1128/mBio.00047-21.

Invited Editor Dominique H. Limoli, University of Iowa

Editor Michael S. Gilmore, Harvard Medical School

Address correspondence to Marvin Whiteley, mwhiteley3@gatech.edu.

Received 11 January 2021
Accepted 25 February 2021
Published 30 March 2021

Polymicrobial infections often cause more damage and are more recalcitrant to clearance than those caused by a single microbe (1–5). Two bacteria commonly found together in human polymicrobial infections are *Pseudomonas aeruginosa* and *Staphylococcus aureus*, which cause chronic infections at a number of body sites in individuals with a variety of comorbidities, including cystic fibrosis (CF) (6, 7). *P. aeruginosa* and *S. aureus* are the two most common bacteria infecting the CF lung, and their coinfection is associated with increased morbidity and mortality (8–11). Experiments in animal models coinoculated with *P. aeruginosa* and *S. aureus* indicate that coinfection increases disease severity and antimicrobial resistance (12–16).

While animal models have provided insights into *P. aeruginosa-S. aureus* coinfections, in many cases the molecular mechanisms controlling enhanced pathogenesis and antimicrobial resistance are not known. One of the challenges to defining coinfection mechanisms is that animal models of infections are constrained in model design, with regard to both the numbers of bacteria required for establishing an infection and the duration of the infection. In addition, time-resolved, simultaneous assessment of bacterial fitness, spatial structure, and function is often not feasible in animal models. This has necessitated the development of versatile, *in vitro* models to discover and molecularly characterize *P. aeruginosa-S. aureus* coculture interaction mechanisms, which can subsequently be studied in animal models. However, developing *in vitro* experimental models has been challenging, as *P. aeruginosa* is highly lytic for *S. aureus* under most *in vitro* coculture conditions (15–23). As a consequence, cocultures are generally stable only when *P. aeruginosa* is at low cell density (22). Given these challenges, work to mechanistically characterize interactions between *P. aeruginosa* and *S. aureus* has often been performed by exposing one bacterium to the cell-free supernatant of the other (24–27). These studies have shown that *P. aeruginosa* antistaphylococcal activity is driven by exoproducts, including proteases and secondary metabolites such as hydrogen cyanide, phenazines, and quinoline *N*-oxides (18, 23, 28–30).

One of the most widely recognized exoproducts of *P. aeruginosa* with potent antistaphylococcal activity is 2-heptyl-4-hydroxyquinoline *N*-oxide (HQNO). HQNO has been found in CF lung exudates and kills *S. aureus* by inhibiting cellular respiration and reducing cellular ATP (23, 31, 32). In addition to its potent antistaphylococcal activity, sublytic levels of HQNO can alter the physiology of *S. aureus* by shifting its metabolism from respiration to fermentation (33), increasing biofilm formation (27), inducing a small-colony variant phenotype (34), and increasing its susceptibility to membrane-targeting antimicrobials, (25) while decreasing its susceptibility to aminoglycosides (24).

While supernatant addition experiments have identified HQNO and other potential interaction mechanisms driven by secreted products, they do not allow study of cell-cell interactions or the spatial organization of the microbial community, both of which impact polymicrobial infection outcomes (35–39). Thus, there is a need for experimental models that allow for stable coculture of *P. aeruginosa* and *S. aureus* in the laboratory. Several studies have developed such systems by altering the bacterial genotype or growth conditions. For example, *in vitro* coexistence has been obtained by using a mucoid strain of *P. aeruginosa* that has less lytic activity against *S. aureus* (40), by exchanging medium and removing planktonic cells to extend coexistence (33), or by altering the frequency of *P. aeruginosa*/*S. aureus* or the growth environment (20, 41). However, laboratory coculture models can be further improved with the explicit goal of mimicking both the chemical and physical environment of the human infection site (2, 42).

In this study, we combined ecological and molecular techniques to understand interactions between *P. aeruginosa* and *S. aureus* in an *in vitro* infection model (synthetic CF sputum medium [SCFM2]) that has been shown to mimic the chemical and physical environment of expectorated CF sputum (17, 21, 43–45). We demonstrated that *S. aureus* and *P. aeruginosa* robustly coexist in SCFM2 under static conditions but not in mixed coculture. Then, using high-resolution confocal microscopy and a computational framework that quantifies spatial structure at the micrometer scale, we found

that HQNO can alter spatial patterning between the two species without altering fitness. Further, we showed that HQNO increases tolerance of *S. aureus* to the aminoglycoside tobramycin in coculture with *P. aeruginosa*.

RESULTS AND DISCUSSION

***P. aeruginosa* and *S. aureus* coexist in static but not well-mixed SCFM2.** The goal of this study was to develop a biologically relevant *in vitro* experimental system that allows the coexistence of *P. aeruginosa* and *S. aureus* and provides the versatility to study their interactions with micrometer-scale spatial resolution. The system we chose was coculture in SCFM2, a defined medium designed by quantifying the chemical composition of sputum expectorated by individuals with CF (45). The gene expression signature of *P. aeruginosa* grown in SCFM2 is more similar to that in CF sputum directly harvested from humans than other CF preclinical models, including a mouse acute lung model (43). *P. aeruginosa* also requires similar genes to grow in SCFM2 and *ex vivo* in expectorated human CF sputum (45). Importantly for this study, SCFM2 contains relevant levels of DNA and mucin, which promotes the natural formation of *P. aeruginosa* aggregates with sizes similar to those observed in the CF lung (17, 44). SCFM2 has also been shown to be a valuable model for studying *S. aureus* CF infection, including understanding how host immune components affect *S. aureus* physiology and gene expression (9, 42). Of note, growth of both *P. aeruginosa* and *S. aureus* in SCFM2 has been performed previously without mixing under static growth conditions (17, 42, 44, 45).

To determine whether these bacteria can stably coexist in SCFM2, laboratory strains of *P. aeruginosa* (PA14) and *S. aureus* (LAC) were coinoculated into SCFM2 at a 1:1 frequency, cultures were incubated statically or mixed with a magnetic stir bar, and bacterial numbers were quantified at 4-h intervals using agar plate counts on selective media. These strains are well-characterized laboratory strains, are highly virulent and antagonistic, have been used to study *P. aeruginosa-S. aureus* interactions (12, 40, 46, 47), and are representative of other pathogenic strains of the same species, thus incorporating clinical relevance into the study. In addition, these strains display gene expression patterns and aggregate sizes in SCFM2 that are similar to those in human expectorated CF sputum (17, 42–44, 48). As these are not highly adapted CF strains, they serve as a model to study potential interactions in early CF disease. There is no doubt that using adapted CF strains would be more relevant. However, our recent studies show that gene expression of CF-adapted strains in SCFM2 is only slightly more representative of that in later CF disease than that of lab strains (43). Thus, our studies will likely have some relevance for understanding later-stage disease.

Our results reveal that, as previously observed, *P. aeruginosa* is highly lytic for *S. aureus* in well-mixed cocultures, reducing *S. aureus* numbers by ~10,000-fold between hours 8 and 12 (Fig. 1A). However, this decrease in *S. aureus* numbers was not observed when cocultures were incubated statically (Fig. 1B). Moreover, both *P. aeruginosa* and *S. aureus* grew to a density in static coculture similar to that in static monoculture (Fig. 1). These results indicate that *P. aeruginosa* and *S. aureus* coexist in SCFM2 when grown under static conditions with no loss of fitness compared to monoculture static growth.

Antistaphylococcal activity in *P. aeruginosa* is higher under well-mixed culture conditions. *P. aeruginosa* produces several secreted antistaphylococcal molecules, and many of these molecules are produced at higher levels in the presence of oxygen (49, 50). Thus, we hypothesized that a primary mechanism promoting stable *P. aeruginosa-S. aureus* coculture under static conditions was decreased production of antistaphylococcal molecules by *P. aeruginosa* due to decreased mixing. To test this hypothesis, cell-free supernatants from *P. aeruginosa* grown in SCFM2 under mixed and static conditions were collected and assessed for the ability to inhibit *S. aureus* growth using a disc diffusion assay (Fig. 1C). For this assay, *P. aeruginosa* supernatant was added to a filter disc on an agar plate containing *S. aureus*, and the zone of inhibition was measured. *P. aeruginosa* grown as a well-mixed culture in SCFM2 produced a zone of

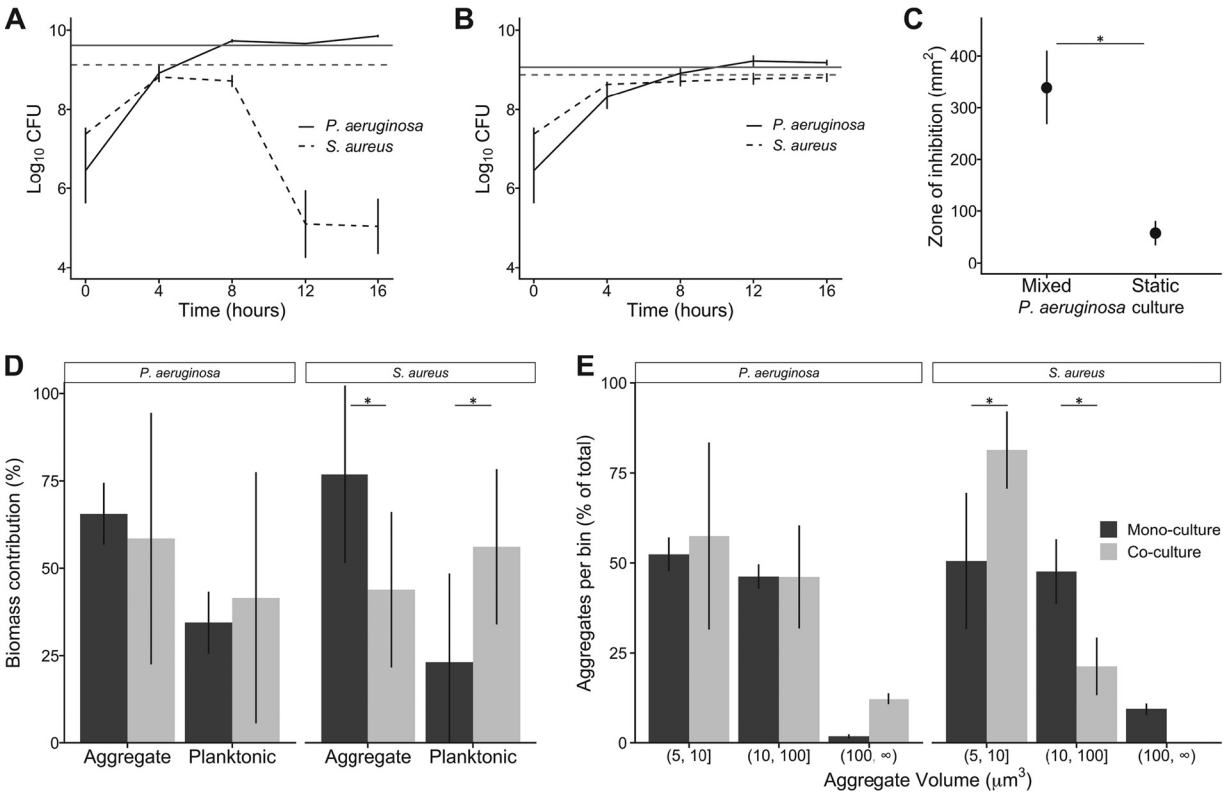

FIG 1 *S. aureus* and *P. aeruginosa* stably coexist in static SCFM2. Growth of *P. aeruginosa* PA14 and *S. aureus* LAC under (A) well-mixed and (B) static conditions in SCFM2 ($n = 3$). Black lines represent CFU in coculture, and the horizontal dark gray lines indicate growth yield after 16 h in monoculture. (C) Normalized zone of inhibition produced by *P. aeruginosa* supernatants spotted on filter discs on lawns of *S. aureus*. *P. aeruginosa* produced a larger zone of inhibition when grown well-mixed in SCFM2 than when grown statically in SCFM2 ($n = 5$, paired Student's *t* test, $P = 1 \times 10^{-3}$). (D) Aggregate and planktonic biomass of *P. aeruginosa* and *S. aureus* in SCFM2 in mono- and coculture. *S. aureus* biomass primarily exists as aggregates in monoculture and as planktonic cells in coculture. Black bars represent monoculture, and gray bars represent coculture ($n = 3$, paired Student's *t* test, $P = 0.02$ for both comparisons). (E) Number of aggregates of *P. aeruginosa* and *S. aureus* within different aggregate size ranges in mono- and coculture. We quantified the number of aggregates in three size ranges: 5 μm^3 to 10 μm^3, 10 μm^3 to 100 μm^3, and larger than 100 μm^3 and reported the percentage of total aggregates in each size range. A lower percentage of aggregates were observed in the 5- to 10-μm^3 range during monoculture than during coculture (50% versus 80%) for *S. aureus* ($n = 3$, paired Student's *t* test, $P = 0.05$), and a correspondingly higher percentage of aggregates in the 10- to 100-μm^3 range were observed in coculture than in monoculture (20% versus 47%) (paired Student's *t* test, $P = 0.03$). Black bars represent monoculture, and gray bars represent coculture. Error bars show standard deviations. (*, $P < 0.05$, paired Student's *t* test.).

inhibition with a diameter more than ~6 times larger than growth in static culture (Fig. 1C). These results reveal that *P. aeruginosa* supernatants from well-mixed cultures possess higher antistaphylococcal activity than those from static cultures.

Our findings that ecological factors (well-mixed and static growth) affect *P. aeruginosa* antistaphylococcal activity and the outcome of *P. aeruginosa-S. aureus* coculture dynamics are fundamentally in agreement with recent work from Niggli and Kummerli (20), which showed that *P. aeruginosa* and *S. aureus* coexist in a laboratory medium that promotes aggregation by embedding in low levels of agar. However, that study did not observe an increase in *P. aeruginosa* relative fitness compared to *S. aureus* during growth in mixed conditions compared to agar conditions, which differs from our observations (Fig. 1A and B). The reason for this is not clear, but it is likely explained by low aeration of the mixed culture condition used by Niggli and Kummerli (20). That study performed mixed coculture in laboratory medium in wells of 24-well plates, using a volume of 1.5 ml in a well with a maximum volume of 3.4 ml and shaking at 170 rpm (20). In our experience, *P. aeruginosa* requires high shaking rates (250 rpm) and low culture volume/culture vessel volume (1/10 to 1/50) for sufficient aeration, and these culture conditions lead to high antistaphylococcal activity (15, 19, 21, 22). Here, we mixed SCFM2 using a stir bar at 250 rpm to ensure high levels of aeration.

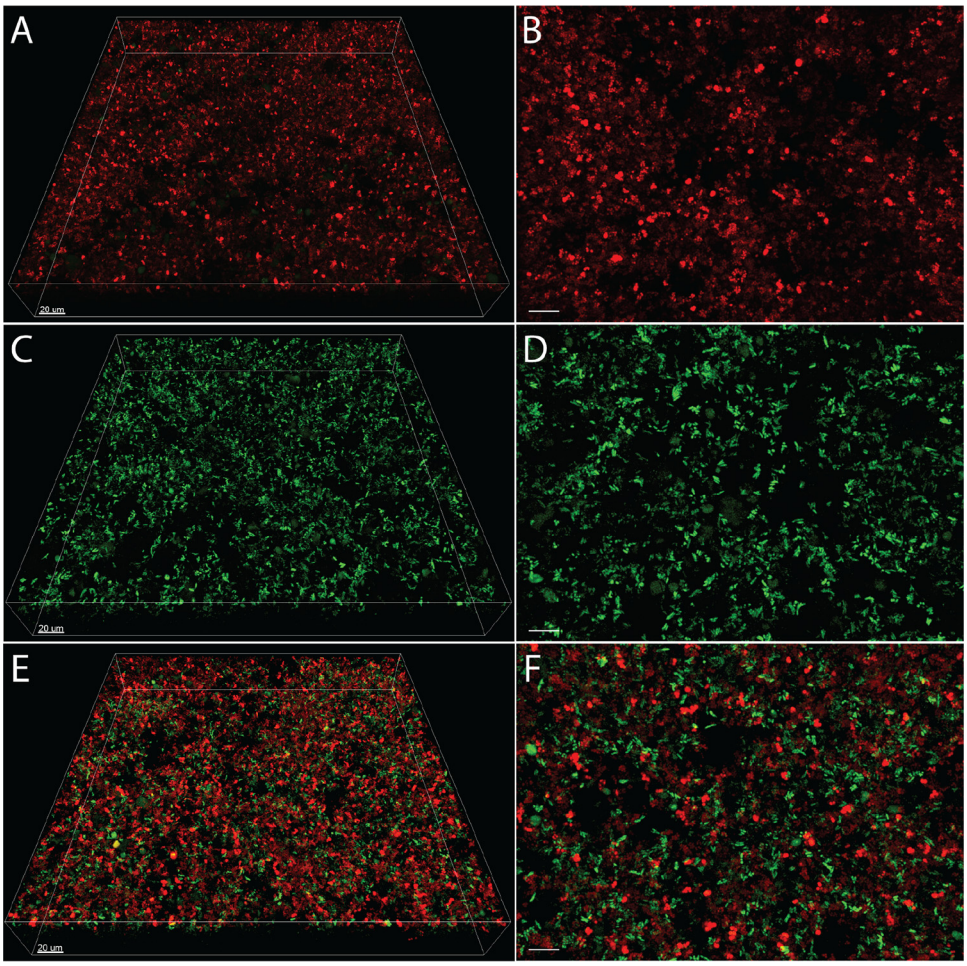

FIG 2 Images of *P. aeruginosa* and *S. aureus* in mono- and coculture in SCFM2. Representative confocal images of DsRed-expressing *S. aureus* LAC (red) in (A and B) monoculture, GFP-expressing *P. aeruginosa* PA14 (green) in monoculture (C and D), and *S. aureus* and *P. aeruginosa* in coculture (E and F). Images on the left (A, C, and E) show the entire imaging field of 270 μm by 270 μm by 40 μm. Images on the right (B, D, and F) show a close-up view of images on the left. Bars, 10 μm unless otherwise noted.

Regardless, both studies agree that *P. aeruginosa* and *S. aureus* coexist in culture conditions that promote aggregation, which restricts movement and promotes the development of spatial structure.

Aggregate sizes and distributions in *P. aeruginosa-S. aureus* mono- and cocultures. The micrometer-scale spatial structure of infecting polymicrobial communities has been shown to affect infection severity in a mouse abscess model (39); thus, one of the goals of this work was to develop a biologically relevant experimental system that allows the spatial structure of *P. aeruginosa* and *S. aureus* to be assessed temporally and at the micrometer scale. Based on the diversity of interactions that have been described, we hypothesized that there would be significant differences in spatial structure of *P. aeruginosa-S. aureus* cocultures compared to monoculture, despite the fact that cell numbers are equivalent (Fig. 1B). To test this hypothesis, we inoculated *P. aeruginosa* expressing the green fluorescent protein (GFP) and *S. aureus* expressing the red fluorescent protein DsRed in mono- and coculture (1:1 frequency) into SCFM2, incubated them statically, and imaged them using confocal laser scanning microscopy (CLSM) (Fig. 2). We chose to end our experiments at 5 h for several reasons: (i) transcriptomic analysis of *P. aeruginosa* at the 5- to 6-h time point in SCFM2 has been shown to most accurately mimic the gene expression of *P. aeruginosa* in human expectorated sputum (43, 48); (ii) transcriptomic analysis of *S. aureus* in SCFM2 at this

time point is also similar to that in human expectorated sputum (42); (iii) *P. aeruginosa* naturally forms aggregates in SCFM2 with sizes similar to those in expectorated CF sputum at this time point (17); (iv) *S. aureus* and *P. aeruginosa* numbers at this time point are within the range often observed in human CF sputum; and (v) *S. aureus* has just reached maximum growth yields at this time point, and DsRed fluorescence fades rapidly as the cells progress deeper into stationary phase. This may be caused by a transcriptional regulation of the *sarA* promoter, which drives DsRed (51).

To quantify the spatial structure of each culture, we utilized a custom computational pipeline (publicly available at https://jupabago.github.io/PaSaProject/) that was recently used to quantify the spatial structure of bacterial communities on human teeth (37). The first step in this pipeline is to discriminate between bacterial cells growing planktonically and those growing as aggregates (biofilms). To accomplish this, we first identified all bacterial objects from CLSM images and classified them by volume, using previously established guidelines defining planktonic cells as objects with a size of $<5\ \mu m^3$ and aggregates as those with a size of $\geq 5\ \mu m^3$ (17). This analysis revealed that *S. aureus* and *P. aeruginosa* are present as both planktonic cells and aggregates in mono- and coculture in SCFM2 (Fig. 1D). However, the percentage of *S. aureus* biomass in aggregates in monoculture (~75%) was twice as high as in coculture, and correspondingly, planktonic cells contributed less to the total biomass in mono- than coculture (Fig. 1D). In contrast, aggregates of *P. aeruginosa* in mono- and coculture contributed equally to total biomass, although the coculture values displayed higher variance (Fig. 1D).

Next, we focused only on the portion of the biomass in aggregates to determine whether coculture impacted aggregate size. We defined bins of increasing aggregate size and quantified the number of *P. aeruginosa* and *S. aureus* aggregates within each bin (Fig. 1E). The bin sizes were chosen to include the most common observed aggregate size range in human expectorated sputum (10 to 100 μm^3) as well as a smaller and a larger bin (17, 52–54). *P. aeruginosa* aggregate size was not affected by the presence of *S. aureus*, with over 95% of aggregates being $\leq 100\ \mu m^3$ in both mono- and coculture. However, *S. aureus* had a higher percentage of aggregates that were $\leq 10\ \mu m^3$ in coculture compared to monoculture (80% versus 50%, respectively) and a correspondingly lower percentage that were between 10 and 100 μm^3 (20% versus 47%).

Collectively, these results reveal that while *P. aeruginosa* and *S. aureus* both exist as aggregates and planktonic cells in mono- and coculture, the *S. aureus* population shifts toward planktonic cells and small aggregates during coculture. The biological relevance of the shift of *S. aureus* to a more planktonic mode during coculture is not known. However, as there is no decrease in fitness in coculture compared to monoculture under static growth conditions (Fig. 1B), it is clear that it is not necessary for *S. aureus* to grow as large aggregate biofilms to be fit in the presence of *P. aeruginosa*. The finding that *P. aeruginosa* exists as both aggregates (65% biomass in monoculture) (Fig. 1D) and planktonic cells (35% biomass in monoculture) (Fig. 1D) in SCFM2 further supports the biological relevance of this model, as recent studies revealed that *P. aeruginosa* exists in expectorated CF sputum as both aggregates (~75% of biomass) and planktonic cells (~25% of biomass) (17, 52, 54).

Impact of HQNO on *P. aeruginosa*-*S. aureus* community structure. As we have now developed a biologically relevant coculture model for studying *P. aeruginosa*-*S. aureus* interactions, we next sought to examine the impact of *P. aeruginosa*-produced HQNO on this community. We chose HQNO as not only does it have antimicrobial activity against *S. aureus*, but also, subinhibitory levels impact the physiology of *S. aureus*, including susceptibility to antimicrobials (24, 25, 27, 33, 34). In addition, the gene encoding the enzyme required for the final step in HQNO biosynthesis (*pqsL*) is expressed similarly in static SCFM2 at the 5-h time point and in human expectorated sputum (43), providing evidence of the biological relevance of SCFM2 for studying HQNO at this time point.

To examine the role of HQNO in community structure, we first created a strain of *P.*

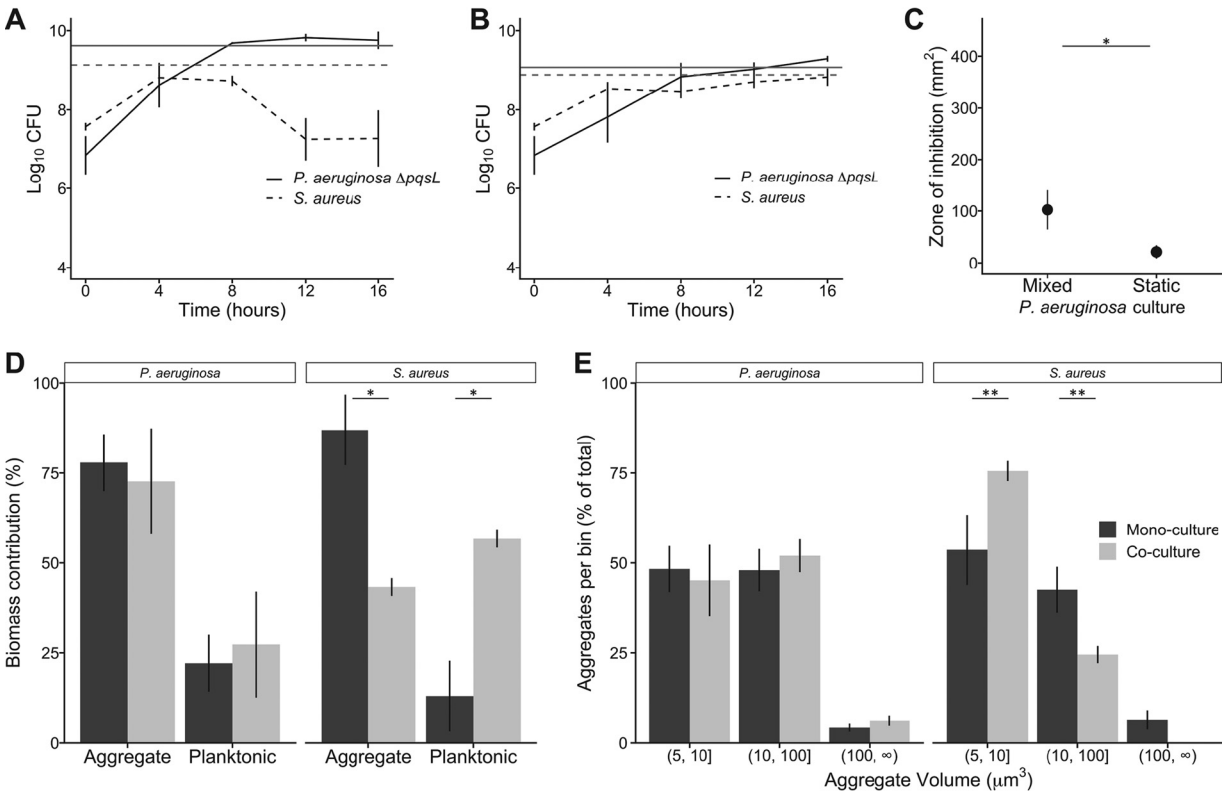

FIG 3 HQNO impacts *S. aureus* fitness in well-mixed but not static SCFM2 cocultures. Growth of *P. aeruginosa* Δ*pqsL* and *S. aureus* under (A) well-mixed and (B) static conditions in SCFM2 ($n = 3$). Black lines represent CFU over time in coculture, and the horizontal dark gray line indicates growth yield after 16 h in monoculture. (C) Zone of inhibition produced by *P. aeruginosa* Δ*pqsL* supernatants spotted on filter discs on lawns of *S. aureus*. *P. aeruginosa* produced a larger zone of inhibition when grown well-mixed in SCFM2 than in static SCFM2 ($n = 5$, paired Student's *t* test, $P = 0.012$) but not as large as wild-type *P. aeruginosa* ($P = 0.023$; Fig. 1C). (D) Aggregate and planktonic biomass of *P. aeruginosa* Δ*pqsL* and *S. aureus* in SCFM2 mono- and coculture. Similar to coculture with wild-type *P. aeruginosa*, *S. aureus* biomass primarily exists as aggregates in monoculture and as planktonic cells in coculture (paired Student's *t* test, $P = 0.02$). *P. aeruginosa* Δ*pqsL* monoculture biomass was also found to be more present as aggregates than as planktonic cells (paired Student's *t* test, $P = 0.02$). (E) Number of aggregates of *P. aeruginosa* Δ*pqsL* and *S. aureus* within different aggregate size ranges in mono- and coculture. We quantified the number of aggregates in three size ranges (5 to 10 μm^3, 10 to 100 μm^3, and larger than 100 μm^3) and reported the percentage of total aggregates in each size range. Fewer aggregates were observed in the 5- to 10-μm^3 range during monoculture than in coculture for *S. aureus* ($n = 3$, paired Student's *t* test, $P = 0.08$), and a corresponding higher percentage of aggregates in the 10- to 100-μm^3 range were observed in the monoculture than in coculture ($n = 3$, paired Student's *t* test, $P = 0.08$). Error bars show standard deviations (*, $P < 0.05$; **, $P < 0.1$ [paired Student's *t* test]).

aeruginosa that does not produce HQNO by deleting *pqsL* (*P. aeruginosa* Δ*pqsL*) and showed that complementation of this strain with *pqsL* in *trans* restored *S. aureus* lytic ability (see Fig. S1 in the supplemental material). Next, we cocultured *S. aureus* under mixed and static conditions with *P. aeruginosa* Δ*pqsL*. Under well-mixed conditions, *P. aeruginosa* Δ*pqsL* lysed *S. aureus*, but to a lesser degree than wild-type *P. aeruginosa*, reducing *S. aureus* numbers by ~100-fold between 8 and 12 h (Fig. 3A). Under static growth conditions, *P. aeruginosa* Δ*pqsL* and *S. aureus* coexisted and reached similar growth yields in both mono- and coculture (Fig. 3B). As expected from the decrease in *S. aureus* levels at late stages of growth, supernatants from *P. aeruginosa* Δ*pqsL* grown as well-mixed cultures exhibited antistaphylococcal activity against *S. aureus*, as observed using the disc diffusion assay (Fig. 3C). This activity was less than that observed for well-mixed wild-type *P. aeruginosa* ($P = 0.023$, Student's *t* test) and similar to that observed for supernatants from static wild-type *P. aeruginosa*. However, supernatants from *P. aeruginosa* Δ*pqsL* grown statically had little antimicrobial activity (Fig. 3C). These data reveal that the antistaphylococcal activity of HQNO has biological importance in well-mixed, but not static, coculture conditions and that HQNO is not the only lytic factor in well-mixed SCFM2 cocultures.

Aggregate sizes and distributions in *P. aeruginosa* Δ*pqsL* and *S. aureus* mono- and cocultures. While HQNO had no effect on *S. aureus* fitness during static coculture, we next assessed whether this molecule impacted *P. aeruginosa* Δ*pqsL* and *S. aureus*

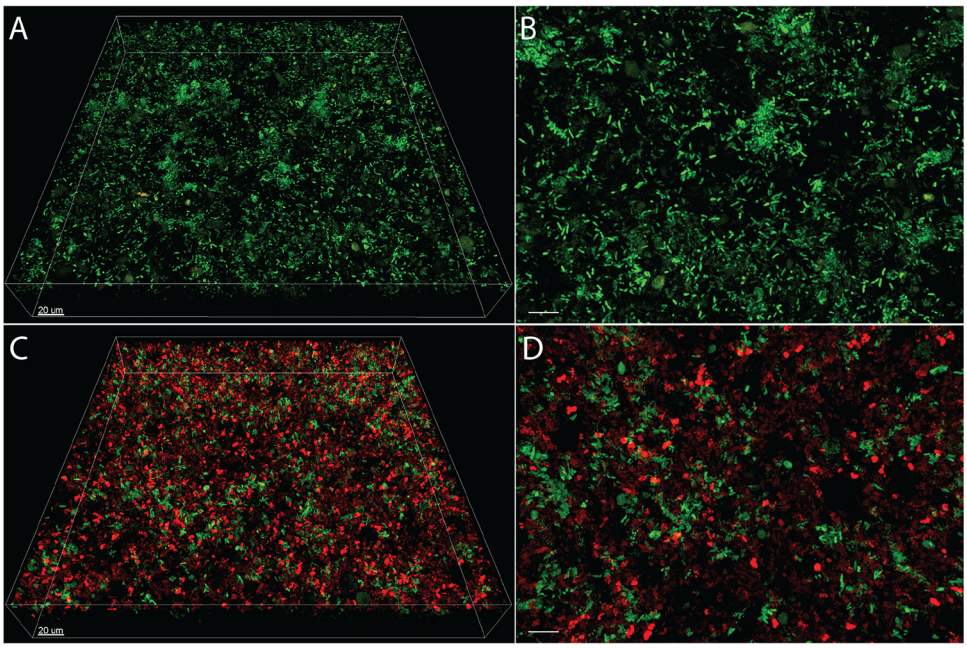

FIG 4 Images of *P. aeruginosa* Δ*pqsL* in mono- and coculture with *S. aureus* in SCFM2. Representative confocal images of GFP-expressing *P. aeruginosa* Δ*pqsL* PA14 (green) in (A and B) monoculture and (C and D) coculture with DsRed-expressing *S. aureus* LAC (red). Images on the left (A and C) show the entire imaging field of 270 μm by 270 μm by 40 μm. Images on the right (B and D) show a close-up view of images on the left. Bars, 10 μm unless otherwise noted.

aggregate number and size using confocal microscopy (Fig. 4), as described above for wild-type *P. aeruginosa-S. aureus* cocultures (Fig. 1D and E). This analysis revealed that cocultures containing *P. aeruginosa* Δ*pqsL* (Fig. 3D) were overall similar to those with wild-type *P. aeruginosa* (Fig. 1D) in regard to aggregate biomass, with *P. aeruginosa* Δ*pqsL* primarily being found as aggregates in both monoculture (77%) and coculture (72%) and *S. aureus* existing primarily as aggregates in monoculture and as planktonic cells in coculture (Fig. 3D). Similar to wild-type *P. aeruginosa*, *P. aeruginosa* Δ*pqsL* aggregate size was not affected by the presence of *S. aureus*, with over 95% of aggregates being $\leq$100 μm^3 in both mono- and coculture (Fig. 3E). In addition, *S. aureus* had a higher percentage of aggregates that were $\leq$10 μm^3 in coculture than in monoculture (75% versus 55%, respectively) and a correspondingly lower percentage that were between 10 and 100 μm^3 (25% versus 40%, respectively). These results reveal that although HQNO is an important contributor to *S. aureus* lysis during well-mixed coculture, it plays no role in *P. aeruginosa* and *S. aureus* aggregate biomass and size during static coculture.

HQNO impacts spatial organization of *P. aeruginosa* and *S. aureus* cocultures. While HQNO had no detectable effect on biomass or aggregate size during coculture, we hypothesized that due to its antimicrobial activity, this molecule would impact the spatial organization of the community by increasing the distance between *P. aeruginosa* and *S. aureus*. To test this hypothesis, we quantified spatial organization of *P. aeruginosa-S. aureus* cocultures using two metrics: coaggregation and enrichment distance.

Coaggregation is a common occurrence in many microbial systems and can be quantified by counting the prevalence of aggregates that contain multiple species (55). To test for coaggregation in the *P. aeruginosa-S. aureus* SCFM2 static cocultures, we quantified the proportion of aggregates that contain both *P. aeruginosa and S. aureus*. Our results reveal that coaggregation does not constitute a significant portion of the total biomass in cocultures containing either wild-type *P. aeruginosa* or *P. aeruginosa* Δ*pqsL*, with 1 to 3% of the total aggregates containing both *P. aeruginosa* and *S.*

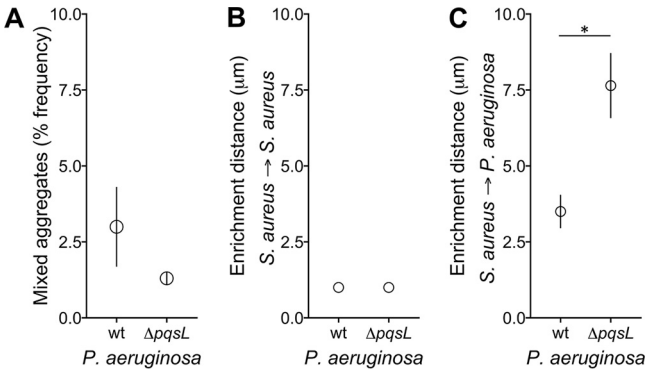

FIG 5 HQNO impacts the spatial organization of *P. aeruginosa* and *S. aureus* communities. (A) Percent mixed-species aggregates of *S. aureus* with *P. aeruginosa* wild-type (wt) and Δ*pqsL* during static growth in SCFM2. (B) Enrichment distance calculated using *S. aureus* as both the focal species and target species, indicating that *S. aureus* is most often found tightly associated with other *S. aureus* cells. (C) Enrichment distance calculated using *S. aureus* as the focal species and *P. aeruginosa* as the target species. *S. aureus* was localized closer to wild-type *P. aeruginosa* than *P. aeruginosa* Δ*pqsL* (paired Student's *t* test, $P = 0.01$). Error bars show standard deviations.

aureus (Fig. 5A). These data indicate that wild-type *P. aeruginosa* and *S. aureus* do not produce substantial numbers of mixed-species aggregates in SCFM2, and the elimination of HQNO does not impact the prevalence of mixed aggregates. These data are also consistent with previous data examining coaggregation of *P. aeruginosa* PA14 strains that express different fluorescent proteins, which revealed that *P. aeruginosa* aggregates primarily arise from single cells (44).

We next asked whether *P. aeruginosa* and *S. aureus* were randomly distributed in SCFM2 or if there was spatial patterning. To answer this question, we characterized spatial patterning of *P. aeruginosa*-*S. aureus* aggregates by calculating enrichment distance. To determine this metric, we first calculated proportional occupancy, which quantifies the composition of the immediate surroundings of a focal community member in relation to other community members at various distance intervals in three dimensions at the micrometer scale (37). Then, enrichment distance was defined as the distance from the focal species at which the proportional occupancy of the target species is the highest. Thus, enrichment distance indicates where biomass of the target species is overrepresented in relation to the focal species. We calculated enrichment distance for cocultures using *S. aureus* as the focal species and *S. aureus* or *P. aeruginosa* as the target species, for both wild-type *P. aeruginosa* and *P. aeruginosa* Δ*pqsL*. In each case, we chose five thousand random DsRed voxels corresponding to *S. aureus* for each replicate and calculated the prevalence of target species voxels within defined distance intervals (30 intervals, each 1 μm). Our results reveal that the enrichment distance of *S. aureus* to *S. aureus* was 0 to 1 μm when cocultured with either the wild-type or Δ*pqsL* strain (Fig. 5B), which is the smallest distance interval tested. These results indicate that on average, an *S. aureus* cell is most often located within 1 μm of a second *S. aureus* cell. These results make intuitive sense and serve as a control for our metric, as a proportion of *S. aureus* in these communities exists in aggregates, which are by definition tightly associated groups of cells. The enrichment distance of *S. aureus* to wild-type *P. aeruginosa* was 3.5 μm, indicating that during static coculture in SCFM2, these two bacteria exist in close proximity to one another (Fig. 5C). Intriguingly, *S. aureus* was on average found at a further distance from *P. aeruginosa* Δ*pqsL* (7.6 μm) than from wild-type *P. aeruginosa*. Thus, although HQNO does not impact the fitness *S. aureus* and *P. aeruginosa* (Fig. 1 and 3), it does affect the spatial structure of the community.

These results are surprising, as we expected that elimination of a potent antimicrobial would allow closer association between *P. aeruginosa* and *S. aureus*. While the

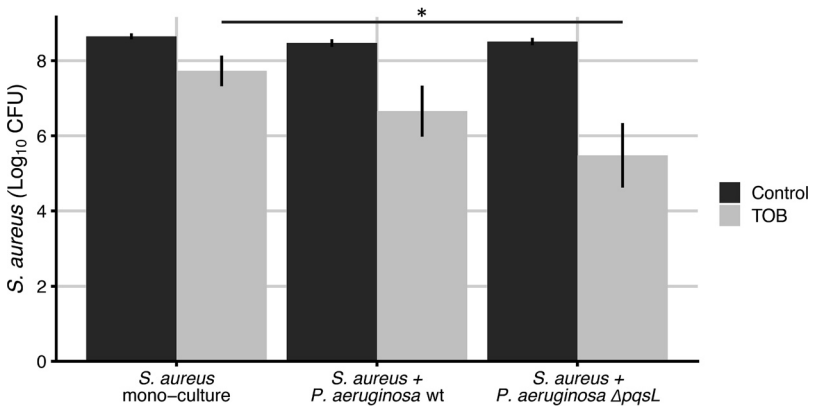

FIG 6 HQNO enhances *S. aureus* survival to tobramycin during coculture. *S. aureus* was grown in SCFM2 under three conditions: monoculture, coculture with *P. aeruginosa*, and coculture with *P. aeruginosa* Δ*pqsL*. Cultures were then treated with tobramycin (256 μg/ml) or water (control), and the number of *S. aureus* CFU was determined. ($n = 12$; *, $P < 0.05$ by the Kruskal-Wallis test, followed by a *post hoc* paired Wilcoxon test). Error bars indicate standard deviations.

mechanism(s) underlying this phenotype is not known, one simple model is competition for molecular oxygen as an electron acceptor. *P. aeruginosa* predominantly respires to generate energy, and while there are low levels of nitrate in SCFM2 that can be used (350 μM), significantly higher levels (50 mM) are needed to support high-yield growth of *P. aeruginosa* in SCFM (56). Thus, O_2 is likely the predominant electron acceptor used during growth in SCFM2. HQNO has been shown to shift *S. aureus* metabolism from respiration to fermentation (33), which may allow close colocalization by preventing competition for O_2. Elimination of HQNO would likely cause competition for O_2, which would lead to *P. aeruginosa* growing in locations where O_2 levels are higher, further from *S. aureus*. Testing this model will require, among other approaches, a technological advancement in micrometer-scale oxygen measurement, which we are currently pursuing using electrochemical approaches.

HQNO enhances tobramycin resistance in *S. aureus* during coculture, although monocultures of *S. aureus* are still more resistant. Previous studies have shown that the presence of HQNO in *P. aeruginosa* supernatants enhances aminoglycoside resistance in *S. aureus* (26). Thus, we used our system to assess whether these findings are also observed in cocultures. We incubated *S. aureus* statically in mono- or coculture with *P. aeruginosa* in SCFM2 for 3 h and then treated the culture with a level of tobramycin (256 μg/ml) that results in 90% killing of monoculture *S. aureus* grown statically in SCFM2 (Fig. 6). Coculture with either wild-type *P. aeruginosa* or the Δ*pqsL* strain increased *S. aureus* susceptibility to tobramycin compared to monoculture (Fig. 6). Further, this increased susceptibility was greatest in coculture with the Δ*pqsL* mutant, which showed a 10-fold decrease in *S. aureus* numbers relative to coculture with wild-type *P. aeruginosa*. These results reveal that similar to previous experiments with *P. aeruginosa* supernatants, HQNO enhances tobramycin resistance of *S. aureus* during coculture with *P. aeruginosa*. However, *S. aureus* monocultures are significantly more resistant to tobramycin killing than cocultures with *P. aeruginosa*, suggesting that ultimately, *P. aeruginosa* sensitizes *S. aureus* to tobramycin killing even in the presence of HQNO. These data are also consistent with recent high-throughput *S. aureus* mutant experiments, which show that *P. aeruginosa* imparts significant stress to *S. aureus* in coinfected murine wounds (13).

Conclusions. Our studies reveal that static growth in SCFM2 allows long-term coculture of *S. aureus* with a strain of *P. aeruginosa* that has high antistaphylococcal activity under well-mixed conditions. Based on this study and our previous findings that SCFM2 is a biologically relevant model for studying CF lung infections (17, 42–45), we propose that this coculture model provides a means to study interactions between *S. aureus*, *P. aeruginosa*, and potentially other bacteria infecting the CF lung. Our results also reveal that elimination of HQNO has no effect on the fitness of *S. aureus* or *P. aeruginosa* during static

coculture relative to monoculture but does impact spatial organization and susceptibility to tobramycin. These data may be particularly meaningful for coculture studies, including those in animals, as bacterial numbers (fitness) are often the primary data used to identify interactions and assess the relevance of specific pathways on bacterial interactions. We propose that assessing spatial organization of communities may be as informative as assessing fitness and that the use of straightforward pipelines for quantifying spatial structure will be critical for understanding the functions of human-associated microbial communities.

While our study focused on laboratory strains of *P. aeruginosa* and *S. aureus*, it is clear that the genotype of the strains used can impact relative fitness during coculture (20, 40, 57). Although we anticipate that relative fitness might be impacted by the use of other strains, as *P. aeruginosa* PA14 is highly lytic for *S. aureus* LAC under well-mixed conditions, their survival in static SCFM2 indicates that this model will likely promote coexistence for multiple genotypes, even those that are highly antagonistic. Finally, it was previously suggested that SCFM2 does not support robust coexistence of *P. aeruginosa* and *S. aureus*, even under static growth conditions (41). However, in the previous study, the static assay quantified bacteria that remained attached to the well of a 96-well plastic dish after vigorous washing, ultimately demonstrating that *P. aeruginosa* was ~100-fold more prevalent than *S. aureus* after 12 h. The likely reason these results differ from ours is that most of the bacteria in SCFM2 grow as suspended aggregates and planktonic cells (17, 44), and we have not focused on the bacteria attached to surfaces, as our goal is to model human infection. In addition, the fact that the previous study observed ~10^7 bacteria attached to the plastic surface at 12 h (41) reveals that only about 1% of the total number of bacteria in the coculture were growing attached to plastic, as the carrying capacity of *P. aeruginosa* in SCFM2 is >10^9 CFU/ml (Fig. 1A and B). Ultimately, our results provide strong evidence that static growth in SCFM2 supports coexistence of *P. aeruginosa* and *S. aureus* and provides the opportunity to study interactions between these common coinhabitants of human infections.

MATERIALS AND METHODS

Strains, media, and growth conditions. Prior to use, strains were streaked on tryptic soy agar plates (Sigma), inoculated into tryptic soy broth, and grown overnight at 37°C with shaking at 250 rpm. Wild-type *P. aeruginosa* strain PA14 and PA14 Δ*pqsL* were fluorescently labeled with the GFP-expressing plasmid pMRP9-1 (58) and maintained with 100 μg/ml of carbenicillin. *S. aureus* LAC was fluorescently labeled by moving pHC48 (59), containing DsRed under the control of the *sarA* promoter, from RN4220 by phage transduction. *S. aureus* carrying pHC48 was cultured with 10 μg/ml of chloramphenicol to maintain the plasmid.

Construction of the *P. aeruginosa* PA14 *pqsL* deletion mutant. A *pqsL* deletion mutant was constructed in PA14 by removing the gene *pqsL* by homologous recombination. The knockout construct was made by amplifying approximately 1-kb DNA fragments upstream and downstream of *pqsL* with overlapping sequences and ligating these fragments into pEXG2 (Promega) using Gibson assembly to form pEXG2pq. Primer sequences to PCR amplify the *pqsL* upstream region were tcggtacccggggatcctctGGTGTTCAACGTGGTCCC and aggaacgctcGCAGCCGTTGATCAGTAC and for amplification of the *pqsL* downstream region were caacggctgcGAGCGTTCCTATCAGCCG and catgcctgcaggtcgactctGTGTTCCTCAATCTGCTGC (capital letters indicate bases that anneal to the *P. aeruginosa* target region, and lowercase corresponds to overhang sequences used for Gibson assembly). For linearizing pEXG2, we used the primers GCTTTACATTTATGCTTCC and ATGATCGTGCTCCTGTCG. The fragments were combined using Gibson assembly, and the resulting ~7-kb plasmid (pEXG2pq) was purified and transformed into *Escherichia coli* DH5α using the transformation and storage solution (TSS) method (60) and selected on 15 μg/ml gentamicin. The plasmid was then purified and transformed into *E. coli* SM10 λ*pir* using the TSS method (60) and selected on 15 μg/ml gentamicin. The knockout vector (pEXG2pq) was conjugated into *P. aeruginosa* as previously described (61). *E. coli* was counterselected using *Pseudomonas* isolation agar plates (Sigma), and *P. aeruginosa* recombinants were selected with 60 μg/ml gentamicin. Forty-eight colonies were screened for sensitivity to sucrose. Allelic replacement was confirmed by PCR and phenotypically by identifying colonies that exhibit autolysis (62).

Complementation of *P. aeruginosa* PA14 Δ*pqsL*. *pqsL* was amplified with the Expand long-template PCR system (Sigma) from *P. aeruginosa* PA14 chromosomal DNA using the forward primer 5′-GAATTCGGAACGACACGGAGACTCATCC-3′ and reverse primer 5′-GAGCTCAGCCGCGCGGAGC-3′. The 1,238-bp amplicon was ligated into the TOPO cloning vector using the TOPO TA cloning kit (Thermo Fisher) to create pTOPO-pqsL. *pqsL* was then removed from pTOPO-pqsL by EcoRI digestion and cloned into EcoRI-digested pBBR1MSC-5 (63). In the resulting plasmid (pBBR1-pqsL), *pqsL* is oriented such that it is transcribed from the *lac* promoter.

Growth in SCFM2. Overnight cultures of *P. aeruginosa* and *S. aureus* were subcultured in SCFM (21) until they reached exponential phase (optical density at 600 nm [OD_{600}] of 0.3 to 0.6). Cultures were

then washed and concentrated in prewarmed SCFM without antibiotics to an OD_{600} of 1.0. These cultures were then used to inoculate each bacterium into SCFM2 at an OD_{600} of 0.05 in mono- or coculture. A 300-μl portion of inoculated SCFM2 was then placed into wells of an 8-well optical chamber (Nunc Lab-Tek chambered cover glass) and incubated statically or well mixed at 37°C. Well-mixed cultures included a magnetic stir bar (1.5 by 8 mm) in each of the wells rotating at 250 rpm. Growth was assessed at 4 h intervals (4, 8, 12, and 16 h) using dilution plating with *P. aeruginosa*- and *S. aureus*-selective media, *Pseudomonas* isolation agar and Baird-Parker agar, respectively.

Disc diffusion assays. For the supernatant assays, *P. aeruginosa* cultures were grown as described above in SCFM2. After 16 h, cultures were centrifuged at 5,000 rpm for 10 min, and supernatants were filtered through a 0.45-μm syringe filter and placed on ice. Overnight cultures of *S. aureus* were spread on brain heart infusion (BHI) plates using sterile swabs, 6-mm filter paper discs were placed onto the agar, and 10 μl of either *P. aeruginosa* supernatant or SCFM2 (as a control) was added to each disc and allowed to dry at room temperature. The zone of inhibition was measured after 24 h of incubation at 37°C. The reported normalized zone of inhibition was calculated by measuring the area of inhibition created by each culture condition and divided by the respective growth yield at that culture condition. To assess lysis by *P. aeruginosa* cells, instead of supernatant being added to a disc, 5 μl of planktonic BHI-grown *P. aeruginosa* ($OD_{600} = 0.5$) was added.

Tobramycin susceptibility assay. *S. aureus* was inoculated as described above in SCFM2 in mono- or coculture with *P. aeruginosa*, grown statically for 3 h, then treated with 256 μg/ml tobramycin for 2 h. Surviving bacteria were quantified by dilution plating with *P. aeruginosa*- and *S. aureus*-selective media, *Pseudomonas* isolation agar and Baird-Parker agar, respectively.

CLSM imaging. The SCFM2 culture method described above was used for imaging. Three wells (*S. aureus* monoculture, *P. aeruginosa* monoculture, and coculture) per optical chamber were used for each replicate imaging experiment. Each experiment imaged a single position in each well, once per hour. All images were acquired with a Zeiss LSM 880 CLSM utilizing Zen image capture software. Detection of DsRed-expressing *S. aureus* cells was performed with an excitation wavelength centered at 587 nm and an emission wavelength centered at 610 nm. Detection of GFP-expressing cells was performed using an excitation wavelength centered at 488 nm and an emission wavelength centered at 509 nm. All images were acquired using a 63× oil-immersion objective. All data were stored as 1,024- by 1,024-pixel slices in stacks of 91 8-bit images. Each voxel is 0.264 by 0.264 by 0.44 μm^3.

Image thresholding. Confocal images were exported as a tiff stack and thresholded using MATLAB (Simulink). A threshold was identified for each image stack using Otsu's method (64). For each channel, the final threshold for all images was identified by calculating a trend line over time across all calculated thresholds and using the value at the median time point.

Calculating aggregate size and histograms. Binarized image stacks were imported as a 3D matrix and segmented using the bwconncomp function (MATLAB R2019a; Simulink), finding connected voxels with 18-level connectivity (identifying voxels that touch at one of their faces or edges). The size of each object was mapped from voxels to cubic micrometers, and a histogram with a 5-μm^3 bin size was created using a custom script in R (version 3.6.1).

Determination of single versus multispecies aggregates. To identify multispecies aggregates, cocultured binarized image slices with *S. aureus* in the red channel and *P. aeruginosa* in the green channel were converted to grayscale images using im2bw function and segmented using the labels function to identify connected pixels in 2 dimensions of bacterial biomass, independent of species (MATLAB R2019a; Simulink). Those bacterial segments create a bacterial objects matrix. Two more matrices were created; one for *P. aeruginosa* (green channel) and another for *S. aureus* (red channel). The bacterial matrix was then combined with either the green or red matrix from the same image to characterize the composition of bacterial segments in regard to species-specific segments. Bacterial aggregates composed of more than one channel were considered multispecies aggregates.

Calculating proportional occupancy and enrichment distance. To determine proportional occupancy, binarized image stacks were analyzed using a custom pipeline developed in R (publicly available at https://jupabago.github.io/PaSaProject/). Briefly, a focal voxel in the 3D image was picked at random and the voxels of a specific channel that were located within a spherical distance interval away (between radius 1 and radius 2) from the focal voxel were counted. Proportional occupancy was calculated by multiplying the number of voxels within a distance interval by the size of each voxel and dividing by the total volume of the spherical shell bound by that distance interval: (number of voxels in distance interval × voxel volume)/total volume of interval.

Proportional occupancy was obtained for 5,000 random focal voxels per image, starting from a distance of 1 μm away from each focal voxel and continuing for 30 μm using 1-μm distance intervals. When the focal voxel picked at random was located closer than 30 μm to the edge of the image, the proportional occupancy was corrected by using the volume of shells from a capped sphere instead of spherical shells. Proportional occupancy was calculated using *S. aureus* as a focal point and using *S. aureus* (control) or *P. aeruginosa* as surrounding cells. For the 5,000 random focal voxels, a histogram of proportional occupancy values was produced at each distance. The proportional occupancy was calculated for each distance interval as the weighted median, and the distance interval with the highest weighted median is the enrichment distance.

SUPPLEMENTAL MATERIAL

Supplemental material is available online only.

FIG S1, TIF file, 2.2 MB.

ACKNOWLEDGMENTS

We acknowledge the Whiteley lab, particularly Gina Lewin, for discussion of the manuscript. We thank Alex Horswill's lab for *S. aureus* fluorescent constructs and Carolyn Ibberson for constructing *S. aureus* LAC pHC48. Additionally, we thank Roman Popat for discussion and idea generation for the spatial organization algorithm.

This work was supported by National Institutes of Health grants R01GM116547 and R56HL142857 (to M.W.) as well as Cystic Fibrosis Foundation grants WHITEL19P0 and WHITEL16G0 (to M.W.). M.W. is a Burroughs Wellcome Investigator in the Pathogenesis of Infectious Disease.

REFERENCES

1. Brogden KA, Guthmiller JM, Taylor CE. 2005. Human polymicrobial infections. Lancet 365:253–255. https://doi.org/10.1016/S0140-6736(05)17745-9.
2. Dalton T, Dowd SE, Wolcott RD, Sun Y, Watters C, Griswold JA, Rumbaugh KP. 2011. An in vivo polymicrobial biofilm wound infection model to study interspecies interactions. PLoS One 6:e27317. https://doi.org/10.1371/journal.pone.0027317.
3. Griffiths EC, Pedersen AB, Fenton A, Petchey OL. 2011. The nature and consequences of coinfection in humans. J Infect 63:200–206. https://doi.org/10.1016/j.jinf.2011.06.005.
4. Murray JL, Connell JL, Stacy A, Turner KH, Whiteley M. 2014. Mechanisms of synergy in polymicrobial infections. J Microbiol 52:188–199. https://doi.org/10.1007/s12275-014-4067-3.
5. Smith H. 1982. The role of microbial interactions in infectious disease. Phil Trans R Soc Lond B Biol Sci 297:551–561.
6. Knapp EA, Fink AK, Goss CH, Sewall A, Ostrenga J, Dowd C, Elbert A, Petren KM, Marshall BC. 2016. The Cystic Fibrosis Foundation Patient Registry. Design and methods of a national observational disease registry. Ann Am Thorac Soc 13:1173–1179. https://doi.org/10.1513/AnnalsATS.201511-781OC.
7. Trivedi U, Parameswaran S, Armstrong A, Burgueno-Vega D, Griswold J, Dissanaike S, Rumbaugh KP. 2014. Prevalence of multiple antibiotic resistant infections in diabetic versus nondiabetic wounds. J Pathog 2014:173053. https://doi.org/10.1155/2014/173053.
8. Hubert D, Réglier-Poupet H, Sermet-Gaudelus I, Ferroni A, Le Bourgeois M, Burgel P-R, Serreau R, Dusser D, Poyart C, Coste J. 2013. Association between *Staphylococcus aureus* alone or combined with *Pseudomonas aeruginosa* and the clinical condition of patients with cystic fibrosis. J Cyst Fibros 12:497–503. https://doi.org/10.1016/j.jcf.2012.12.003.
9. Emerson J, Rosenfeld M, McNamara S, Ramsey B, Gibson RL. 2002. Pseudomonas aeruginosa and other predictors of mortality and morbidity in young children with cystic fibrosis. Pediatr Pulmonol 34:91–100. https://doi.org/10.1002/ppul.10127.
10. Zhao J, Schloss PD, Kalikin LM, Carmody LA, Foster BK, Petrosino JF, Cavalcoli JD, VanDevanter DR, Murray S, Li JZ, Young VB, LiPuma JJ. 2012. Decade-long bacterial community dynamics in cystic fibrosis airways. Proc Natl Acad Sci U S A 109:5809–5814. https://doi.org/10.1073/pnas.1120577109.
11. Goss CH, Muhlebach MS. 2011. Staphylococcus aureus and MRSA in cystic fibrosis. J Cyst Fibros 10:298–306. https://doi.org/10.1016/j.jcf.2011.06.002.
12. Cigana C, Bianconi I, Baldan R, De Simone M, Riva C, Sipione B, Rossi G, Cirillo DM, Bragonzi A. 2018. *Staphylococcus aureus* impacts *Pseudomonas aeruginosa* chronic respiratory disease in murine models. J Infect Dis 217:933–942. https://doi.org/10.1093/infdis/jix621.
13. Ibberson CB, Stacy A, Fleming D, Dees JL, Rumbaugh K, Gilmore MS, Whiteley M. 2017. Co-infecting microorganisms dramatically alter pathogen gene essentiality during polymicrobial infection. Nature Microbiol 2:17079. https://doi.org/10.1038/nmicrobiol.2017.79.
14. Korgaonkar A, Trivedi U, Rumbaugh KP, Whiteley M. 2013. Community surveillance enhances *Pseudomonas aeruginosa* virulence during polymicrobial infection. Proc Natl Acad Sci U S A 110:1059–1064. https://doi.org/10.1073/pnas.1214550110.
15. Mashburn LM, Jett AM, Akins DR, Whiteley M. 2005. *Staphylococcus aureus* serves as an iron source for *Pseudomonas aeruginosa* during in vivo coculture. J Bacteriol 187:554–566. https://doi.org/10.1128/JB.187.2.554-566.2005.
16. Millette G, Langlois J-P, Brouillette E, Frost EH, Cantin A, Malouin F. 2019. Despite antagonism in vitro, *Pseudomonas aeruginosa* enhances *Staphylococcus aureus* colonization in a murine lung infection model. Front Microbiol 10:2880. https://doi.org/10.3389/fmicb.2019.02880.
17. Darch SE, Kragh KN, Abbott EA, Bjarnsholt T, Bull JJ, Whiteley M. 2017. Phage inhibit pathogen dissemination by targeting bacterial migrants in a chronic infection model. mBio 8:e00240-17. https://doi.org/10.1128/mBio.00240-17.
18. Kessler E, Safrin M, Olson J, Ohman D. 1993. Secreted LasA of *Pseudomonas aeruginosa* is a staphylolytic protease. J Biol Chem 268:7503–7508. https://doi.org/10.1016/S0021-9258(18)53203-8.
19. Mashburn LM, Whiteley M. 2005. Membrane vesicles traffic signals and facilitate group activities in a prokaryote. Nature 437:422–425. https://doi.org/10.1038/nature03925.
20. Niggli S, Kummerli R. 2020. Strain background, species frequency and environmental conditions are important in determining population dynamics and species co-existence between *Pseudomonas aeruginosa* and *Staphylococcus aureus*. Appl Environ Microbiol 86:e00962-20. https://doi.org/10.1128/AEM.00962-20.
21. Palmer KL, Aye LM, Whiteley M. 2007. Nutritional cues control *Pseudomonas aeruginosa* multicellular behavior in cystic fibrosis sputum. J Bacteriol 189:8079–8087. https://doi.org/10.1128/JB.01138-07.
22. Palmer KL, Mashburn LM, Singh PK, Whiteley M. 2005. Cystic fibrosis sputum supports growth and cues key aspects of *Pseudomonas aeruginosa* physiology. J Bacteriol 187:5267–5277. https://doi.org/10.1128/JB.187.15.5267-5277.2005.
23. Machan ZA, Taylor GW, Pitt TL, Cole PJ, Wilson R. 1992. 2-Heptyl-4-hydroxyquinoline N-oxide, an antistaphylococcal agent produced by *Pseudomonas aeruginosa*. J Antimicrob Chemother 30:615–623. https://doi.org/10.1093/jac/30.5.615.
24. Orazi G, O'Toole GA. 2017. *Pseudomonas aeruginosa* alters *Staphylococcus aureus* sensitivity to vancomycin in a biofilm model of cystic fibrosis infection. mBio 8:e00873-17. https://doi.org/10.1128/mBio.00873-17.
25. Orazi G, Ruoff KL, O'Toole GA. 2019. *Pseudomonas aeruginosa* increases the sensitivity of biofilm-grown *Staphylococcus aureus* to membrane-targeting antiseptics and antibiotics. mBio 10:e01501-19. https://doi.org/10.1128/mBio.01501-19.
26. Radlinski L, Rowe SE, Kartchner LB, Maile R, Cairns BA, Vitko NP, Gode CJ, Lachiewicz AM, Wolfgang MC, Conlon BP. 2017. *Pseudomonas aeruginosa* exoproducts determine antibiotic efficacy against *Staphylococcus aureus*. PLoS Biol 15:e2003981. https://doi.org/10.1371/journal.pbio.2003981.
27. Fugère A, Lalonde Séguin D, Mitchell G, Déziel E, Dekimpe V, Cantin AM, Frost E, Malouin F. 2014. Interspecific small molecule interactions between clinical isolates of *Pseudomonas aeruginosa* and *Staphylococcus aureus* from adult cystic fibrosis patients. PLoS One 9:e86705. https://doi.org/10.1371/journal.pone.0086705.
28. Park JH, Lee JH, Cho MH, Herzberg M, Lee J. 2012. Acceleration of protease effect on *Staphylococcus aureus* biofilm dispersal. FEMS Microbiol Lett 335:31–38. https://doi.org/10.1111/j.1574-6968.2012.02635.x.
29. Castric PA. 1975. Hydrogen cyanide, a secondary metabolite of *Pseudomonas aeruginosa*. Can J Microbiol 21:613–618. https://doi.org/10.1139/m75-088.
30. Hassan HM, Fridovich I. 1980. Mechanism of the antibiotic action pyocyanine. J Bacteriol 141:156–163. https://doi.org/10.1128/JB.141.1.156-163.1980.
31. Mitchell G, Séguin D, Asselin A-E, Déziel E, Cantin AM, Frost EH, Michaud S, Malouin F. 2010. *Staphylococcus aureus* sigma B-dependent emergence of small-colony variants and biofilm production following exposure to *Pseudomonas aeruginosa* 4-hydroxy-2-heptylquinoline-N-oxide. BMC Microbiol 10:33. https://doi.org/10.1186/1471-2180-10-33.

32. Lightbown J, Jackson F. 1956. Inhibition of cytochrome systems of heart muscle and certain bacteria by the antagonists of dihydrostreptomycin: 2-alkyl-4-hydroxyquinoline N-oxides. Biochem J 63:130–137. https://doi.org/10.1042/bj0630130.
33. Filkins LM, Graber JA, Olson DG, Dolben EL, Lynd LR, Bhuju S, O'Toole GA. 2015. Coculture of *Staphylococcus aureus* with *Pseudomonas aeruginosa* drives *S. aureus* towards fermentative metabolism and reduced viability in a cystic fibrosis model. J Bacteriol 197:2252–2264. https://doi.org/10.1128/JB.00059-15.
34. Hoffman LR, Déziel E, d'Argenio DA, Lépine F, Emerson J, McNamara S, Gibson RL, Ramsey BW, Miller SI. 2006. Selection for *Staphylococcus aureus* small-colony variants due to growth in the presence of *Pseudomonas aeruginosa*. Proc Natl Acad Sci U S A 103:19890–19895. https://doi.org/10.1073/pnas.0606756104.
35. Jiang X, Zerfaß C, Feng S, Eichmann R, Asally M, Schäfer P, Soyer OS. 2018. Impact of spatial organization on a novel auxotrophic interaction among soil microbes. ISME J 12:1443–1456. https://doi.org/10.1038/s41396-018-0095-z.
36. Ratzke C, Gore J. 2016. Self-organized patchiness facilitates survival in a cooperatively growing *Bacillus subtilis* population. Nature Microbiol 1:16022. https://doi.org/10.1038/nmicrobiol.2016.22.
37. Kim D, Barraza JP, Arthur RA, Hara A, Lewis K, Liu Y, Scisci EL, Hajishengallis E, Whiteley M, Koo H. 2020. Spatial mapping of polymicrobial communities reveals a precise biogeography associated with human dental caries. Proc Natl Acad Sci U S A 117:12375–12386. https://doi.org/10.1073/pnas.1919099117.
38. Stacy A, McNally L, Darch SE, Brown SP, Whiteley M. 2016. The biogeography of polymicrobial infection. Nat Rev Microbiol 14:93–105. https://doi.org/10.1038/nrmicro.2015.8.
39. Stacy A, Everett J, Jorth P, Trivedi U, Rumbaugh KP, Whiteley M. 2014. Bacterial fight-and-flight responses enhance virulence in a polymicrobial infection. Proc Natl Acad Sci U S A 111:7819–7824. https://doi.org/10.1073/pnas.1400586111.
40. Limoli DH, Whitfield GB, Kitao T, Ivey ML, Davis MR, Grahl N, Hogan DA, Rahme LG, Howell PL, O'Toole GA, Goldberg JB. 2017. *Pseudomonas aeruginosa* alginate overproduction promotes coexistence with *Staphylococcus aureus* in a model of cystic fibrosis respiratory infection. mBio 8:e00186-17. https://doi.org/10.1128/mBio.00186-17.
41. Cendra MDM, Blanco-Cabra N, Pedraz L, Torrents E. 2019. Optimal environmental and culture conditions allow the in vitro coexistence of *Pseudomonas aeruginosa* and *Staphylococcus aureus* in stable biofilms. Sci Rep 9:16284. https://doi.org/10.1038/s41598-019-52726-0.
42. Ibberson CB, Whiteley M. 2019. The *Staphylococcus aureus* transcriptome during cystic fibrosis lung infection. mBio 10:e02774-19. https://doi.org/10.1128/mBio.02774-19.
43. Cornforth DM, Diggle FL, Melvin JA, Bomberger JM, Whiteley M. 2020. Quantitative framework for model evaluation in microbiology research using *Pseudomonas aeruginosa* and cystic fibrosis infection as a test case. mBio 11:e03042-19. https://doi.org/10.1128/mBio.03042-19.
44. Darch SE, Simoska O, Fitzpatrick M, Barraza JP, Stevenson KJ, Bonnecaze RT, Shear JB, Whiteley M. 2018. Spatial determinants of quorum signaling in a *Pseudomonas aeruginosa* infection model. Proc Natl Acad Sci U S A 115:4779–4784. https://doi.org/10.1073/pnas.1719317115.
45. Turner KH, Wessel AK, Palmer GC, Murray JL, Whiteley M. 2015. Essential genome of *Pseudomonas aeruginosa* in cystic fibrosis sputum. Proc Natl Acad Sci U S A 112:4110–4115. https://doi.org/10.1073/pnas.1419677112.
46. Briaud P, Camus L, Bastien S, Doleans-Jordheim A, Vandenesch F, Moreau K. 2019. Coexistence with *Pseudomonas aeruginosa* alters *Staphylococcus aureus* transcriptome, antibiotic resistance and internalization into epithelial cells. Sci Rep 9:16564. https://doi.org/10.1038/s41598-019-52975-z.
47. Limoli DH, Warren EA, Yarrington KD, Donegan NP, Cheung AL, O'Toole GA. 2019. Interspecies interactions induce exploratory motility in *Pseudomonas aeruginosa*. Elife 8:e47365. https://doi.org/10.7554/eLife.47365.
48. Cornforth DM, Dees JL, Ibberson CB, Huse HK, Mathiesen IH, Kirketerp-Moller K, Wolcott RD, Rumbaugh KP, Bjarnsholt T, Whiteley M. 2018. *Pseudomonas aeruginosa* transcriptome during human infection. Proc Natl Acad Sci U S A 115:E5125–E5134. https://doi.org/10.1073/pnas.1717525115.
49. Pallett R, Leslie LJ, Lambert PA, Milic I, Devitt A, Marshall LJ. 2019. Anaerobiosis influences virulence properties of *Pseudomonas aeruginosa* cystic fibrosis isolates and the interaction with *Staphylococcus aureus*. Sci Rep 9:6748. https://doi.org/10.1038/s41598-019-42952-x.
50. Schertzer JW, Brown SA, Whiteley M. 2010. Oxygen levels rapidly modulate *Pseudomonas aeruginosa* social behaviours via substrate limitation of PqsH. Mol Microbiol 77:1527–1538. https://doi.org/10.1111/j.1365-2958.2010.07303.x.
51. Bayer MG, Heinrichs JH, Cheung AL. 1996. The molecular architecture of the sar locus in *Staphylococcus aureus*. J Bacteriol 178:4563–4570. https://doi.org/10.1128/jb.178.15.4563-4570.1996.
52. Bjarnsholt T, Alhede M, Alhede M, Eickhardt-Sorensen SR, Moser C, Kuhl M, Jensen PO, Hoiby N. 2013. The in vivo biofilm. Trends Microbiol 21:466–474. https://doi.org/10.1016/j.tim.2013.06.002.
53. DePas WH, Starwalt-Lee R, Van Sambeek L, Ravindra Kumar S, Gradinaru V, Newman DK. 2016. Exposing the three-dimensional biogeography and metabolic states of pathogens in cystic fibrosis sputum via hydrogel embedding, clearing, and rRNA labeling. mBio 7:e00796-16. https://doi.org/10.1128/mBio.00796-16.
54. Kragh KN, Alhede M, Jensen PO, Moser C, Scheike T, Jacobsen CS, Seier Poulsen S, Eickhardt-Sorensen SR, Trostrup H, Christoffersen L, Hougen HP, Rickelt LF, Kuhl M, Hoiby N, Bjarnsholt T. 2014. Polymorphonuclear leukocytes restrict growth of *Pseudomonas aeruginosa* in the lungs of cystic fibrosis patients. Infect Immun 82:4477–4486. https://doi.org/10.1128/IAI.01969-14.
55. Rickard AH, Gilbert P, High NJ, Kolenbrander PE, Handley PS. 2003. Bacterial coaggregation: an integral process in the development of multi-species biofilms. Trends Microbiol 11:94–100. https://doi.org/10.1016/s0966-842x(02)00034-3.
56. Palmer KL, Brown SA, Whiteley M. 2007. Membrane-bound nitrate reductase is required for anaerobic growth in cystic fibrosis sputum. J Bacteriol 189:4449–4455. https://doi.org/10.1128/JB.00162-07.
57. Speare L, Smith S, Salvato F, Kleiner M, Septer AN. 2020. Environmental viscosity modulates interbacterial killing during habitat transition. mBio 11:e03060-19. https://doi.org/10.1128/mBio.03060-19.
58. Davies DG, Parsek MR, Pearson JP, Iglewski BH, Costerton JW, Greenberg EP. 1998. The involvement of cell-to-cell signals in the development of a bacterial biofilm. Science 280:295–298. https://doi.org/10.1126/science.280.5361.295.
59. Ibberson CB, Parlet CP, Kwiecinski J, Crosby HA, Meyerholz DK, Horswill AR. 2016. Hyaluronan modulation impacts *Staphylococcus aureus* biofilm infection. Infect Immun 84:1917–1929. https://doi.org/10.1128/IAI.01418-15.
60. Chung CT, Niemela SL, Miller RH. 1989. One-step preparation of competent *Escherichia coli*: transformation and storage of bacterial cells in the same solution. Proc Natl Acad Sci U S A 86:2172–2175. https://doi.org/10.1073/pnas.86.7.2172.
61. Whiteley M, Lee KM, Greenberg EP. 1999. Identification of genes controlled by quorum sensing in *Pseudomonas aeruginosa*. Proc Natl Acad Sci U S A 96:13904–13909. https://doi.org/10.1073/pnas.96.24.13904.
62. D'Argenio DA, Calfee MW, Rainey PB, Pesci EC. 2002. Autolysis and autoaggregation in *Pseudomonas aeruginosa* colony morphology mutants. J Bacteriol 184:6481–6489. https://doi.org/10.1128/jb.184.23.6481-6489.2002.
63. Kovach ME, Elzer PH, Hill DS, Robertson GT, Farris MA, Roop RM, 2nd, Peterson KM. 1995. Four new derivatives of the broad-host-range cloning vector pBBR1MCS, carrying different antibiotic-resistance cassettes. Gene 166:175–176. https://doi.org/10.1016/0378-1119(95)00584-1.
64. Otsu N. 1979. A threshold selection method from gray-level histograms. IEEE Trans Syst Man Cybern 9:62–66. https://doi.org/10.1109/TSMC.1979.4310076.